Heat Mass Transfer (2009) 45:1617–1625
DOI 10.1007/s00231-009-0536-3

ORIGINAL

Optimal design of angled rib turbulators in a cooling channel

Kyung Min Kim · Hyun Lee · Beom Seok Kim · Sangwoo Shin · Dong Hyun Lee · Hyung Hee Cho

Received: 11 November 2008 / Accepted: 3 September 2009 / Published online: 17 September 2009

Abstract In the present study, an optimal design for enhancement of heat transfer and thermal performance for a stationary channel with angled rib turbulators was investigated to find the most suitable rib geometry. Among various design parameters, two design variables, rib angle of attack (α) and pitch-to-rib height (p/e), were chosen. The ranges of two design variables were set as $30° \leq \alpha \leq 80°$ and $3.0 \leq p/e \leq 15.0$. Approximations for design of the best rib turbulators were obtained using the advanced response surface method with functional variables. The second-order response surfaces (or correlations) within the ranges of two design variables were completed by this method. As for the optimized results, maximum averaged heat transfer value was obtained at $\alpha = 53.31°$ and $p/e = 6.50$, while the highest thermal performance value was presented at $\alpha = 54.67°$ and $p/e = 6.80$.

List of symbols

AR	Channel aspect ratio (W/H)
D_h	Hydraulic diameter (m)
e	Rib height (m)
f	Friction factor
h	Heat transfer coefficient (W m^{-2} K^{-1})
H	Channel height (m)
k_c	Conductivity of air
Nu	Nusselt number (hD_h/k_c)
OF	Objective function
p	Rib-to-rib pitch
Pr	Prandtl number ($\mu C_p/k_c$)
R^2	Determine R square
R^2_{adj}	Adjusted determine R square
Re	Reynolds number, $D_h\, u_b/v$
TP	Thermal performance
u_b	Passage inlet averaged bulk velocity (m s^{-1})
w	Rib width (m)
W	Width of channel (m)
x	Coordinate and distance in the streamwise direction (m)
y	Coordinate and distance in the lateral direction (m)
z	Coordinate and distance in the vertical direction (m)
α	Rib angle of attack
β	Coefficient of polynomial
μ	Dynamic viscosity (kg m^{-1} s^{-1})
ρ	Air density
v	Kinematic viscosity (m^2 s^{-1})

K. M. Kim · H. Lee · B. S. Kim · S. Shin · D. H. Lee · H. H. Cho (✉)
Department of Mechanical Engineering, Yonsei University, Seoul 120-749, Korea
e-mail: hhcho@yonsei.ac.kr

1 Introduction

To improve thermal efficiency of a gas-turbine engine, turbine inlet temperature has been steadily increased that it results in high thermal loads on turbine blades. Thus, effective cooling system design has become crucial for performance enhancement and gas-turbine engine protection. Various cooling schemes (e.g. internal passage cooling, film cooling, and impingement cooling) have been employed to protect blade materials from exceeding the maximum allowable temperature.

Among such cooling methods, the internal passage cooling technique effectively protects gas turbine blades because it covers most of the blade surfaces with minimal loss of the coolant fluid. In general, surface of internal

passage in gas turbine blades is roughened by rib turbulators. These rib turbulators break boundary layers, increase turbulence intensity, induce reattachment flow and create secondary (or swirling) flow structure. These result in significant heat transfer enhancement in the cooling passage. The impingement effect of the secondary flow induced by angled rib turbulators is one of the principal factors for heat transfer enhancement in the cooling passage.

Numerous experiments have been conducted on the angled rib turbulators in stationary channels. Han et al. [1] and Cho et al. [2] reported that the high heat transfer at 60° angle of attack and the high thermal performance at 45° angle of attack are presented. Furthermore, to clarify the effects of secondary flow on heat transfer and pressure drop characteristics in a stationary duct, Taslim et al. [3], Rau et al. [4] and Cho et al. [2] investigated various factors such as rib height (e), rib angle of attack (α), rib shape, rib arrangement, and discrete ribs. In the other works, Astarita et al. [5], Lau et al. [6], Kim et al. [7, 8] also investigated each individual effect such as duct shape, rib shape, rib arrangement and channel rotation in cooling channels with angled rib turbulators.

As aforementioned, most of the previous studies have dealt with heat transfer characteristics in angled ribbed channels with a ratio of rib-to-rib pitch to rib height (p/e) ratio higher than 8.0, since it is well-known that the highest heat transfer performance appears when the ratio (p/e) is between 8.0 and 10.0 in a 90° ribbed channel through early experiments of Han et al. [9] and Berger et al. [10]. In the most resent, Liu [11] found that the heat transfer is high at short p/e under their experiments. They reported that the reason being is that the angled rib-induced secondary flow effectively mixes with the circulation flow which is presented among the inter-rib turbulators with the short rib-to-rib pitch. However, at some short rib-to-rib pitch, heat transfer could become lower than that at long rib-to-rib pitch.

Therefore, finding out the rib-to-rib pitches with the highest heat transfer and thermal performance is important for optimal rib design. Furthermore, since the rib angle of attack affects the actual rib-to-rib pitch, the combined effects of the rib angle of attack and rib-to-rib pitch should be studied. In the prior studies, Kim et al. [12, 13] used the general response surface method based on dimensionless design variables for optimizing the shape of the ribbed channels. They found that this method was suitable to choose the best rib geometry for heat transfer enhancement. However, they obtained an optimal shape at rib-to-rib pitches longer than 10.0 using the general method, which has limitations such as the narrow design variable ranges and low physical response. Due to these limitations, the obtained optimum results had discrepancy from the previous experimental results reported by many researchers.

Therefore, the objective of the current study is to determine the rib-to-rib pitch and angle of attack that yield a maximum heat transfer and a maximum thermal performance using an advanced response method based on the functional design variables with broader design variable ranges and higher physical response compared to the general response surface method. For analysis of heat transfer and friction loss, we employed numerical computations using a commercial package (FLUENT 6.2). From the resultant values, we obtained the second-order correlations with functional design variables and thereby rib geometries with maximum heat transfer and maximum thermal performance.

2 Research methods

2.1 Numerical analysis of fluid flow and heat transfer

In the present study, all calculations used FLUENT v6.2. The Reynolds-averaged Navier–Stokes equations and the transport equations of the turbulent quantities are solved by the pressure correction algorithm SIMPLE. The fluid is considered to be incompressible and fluid properties are assumed to be constant.

RNG k-ε model is chosen as the turbulence model. The RNG k-ε model is similar in form to the standard k-ε model, but includes the following refinements as described in FLUENT User's Guide [14]: (1) Improvement of the accuracy for rapidly strained flows; (2) Enhancement of accuracy for swirling flows by the effect of swirl on turbulence; (3) Use of an analytical formula for turbulent Prandtl numbers; (4) Use of an analytically-derived differential formula for effective viscosity that accounts for low-Reynolds-number effects. However, effective use of this feature depend on an appropriate treatment of the near-wall region. For these features, the RNG k-ε model is more accurate and reliable for a wider class of flows than the standard k-ε model.

Enhanced wall treatment is chosen for the wall function. Enhanced wall treatment is a near-wall modeling method that combines a two-layer model with enhanced wall function. In general, enhanced wall treatments in the k-ε models are used. It is the same to wall boundary conditions treated in the k-ω models. Although k-ε model is used, the enhanced wall treatment method is available as low-Reynolds-number models as well as high-Reynolds-number models. The grid consists of about 800,000 computational cells for the calculations. To resolve the laminar sublayer computation for enhanced wall treatment, first grid points are calculated to satisfy y^+ less than 1.0 [14].

Figure 1 shows the three dimensional channel with two rib roughed walls. It is a general geometry in order to apply

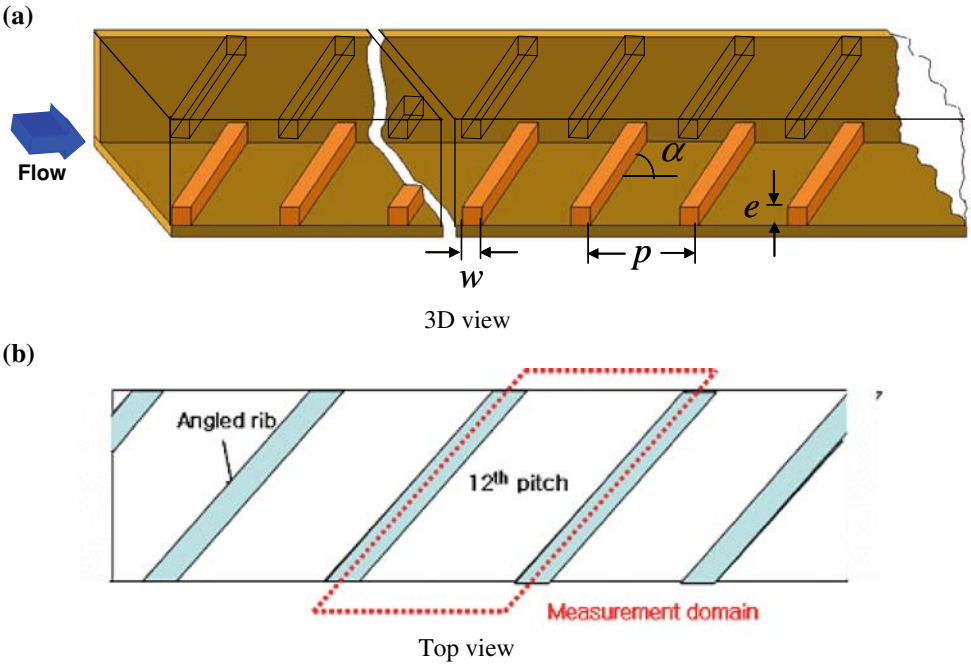

Fig. 1 Geometric parameters and design variables

to heat exchangers, internal cooling of gas turbines, solar heater, etc. The channel has a square cross-section with a hydraulic diameter, $D_h = 40$ mm. It has 15 pitches (irrespective of rib-to-rib distance) for calculating heat transfer coefficients in fully developed flow. The reason is that the flow is fully developed generally after five pitches. In addition, the geometrical dimensions in the present study are the same to those in the experimental study [8]. For the thermal calculation, the wall temperature is specified on channel walls among the angled ribs except rib surfaces. The wall temperature was set to a constant value of 123 K above the bulk inlet temperature of 273 K and bulk velocity corresponding to a Reynolds number of 10,000. Channel outlet flow was set to a pressure outlet condition. Turbulence intensity was 5%. The other geometrical dimensions and the boundary conditions are listed in Table 1.

Table 1 Boundary conditions and parameters

Hydraulic diameter (D_h)	40.0 mm
Channel height (H)	40.0 mm
Channel width (W)	40.0 mm
Number of pitches	15
Rib height	2.2 mm
Rib width	2.2 mm
Inlet averaged bulk velocity (u_b)	3.6457 m/s
Wall temperature	423 K
Inlet temperature	300 K
Turbulence intensity	5%

2.2 Optimization technique (advanced response surface method)

In the engineering design, it is very important to determine the optimum dimensions among many design parameters. Gradient-based optimization, neural network-based response surface method (RSM), Polynomial-based RSM, and genetic algorithm are generally used in many antual fields. Among the optimization methods, the polynomial-based RSM is a well-known optimization technique. This method has the advantage of obtaining a correlation between the design variables, which is applied for selecting the design geometries with an optimum value. Response surface method is to collect results from experiments or numerical analyses of design points, and then to construct a response surface of the quantity over the design space. When the second-order polynomial of two variables is used, the response surface is expressed as follows:

$$y = C_1 x_1^2 + C_2 x_2^2 + C_3 x_1 x_2 + C_4 x_1 + C_5 x_2 + C_6 \quad (1)$$

In general, the equations (such as first or second order polynomials) are used for the response surface based on approximation. These equations can search for the local optimum values within the region of interest as reported by Myers et al. [15]. However, the general response surface method has the disadvantages of inappropriate application to complex functions (more than second order), low physical response (local sensitivity) and selection of design variable ranges. In the other hands, the line resulted from the thermal characteristic of each variable is not to be expressed as a second-order parabola. In effort to solve these problems,

Giunta [16] and Kim [17] proposed an advanced method which is based on functional variables with physical and thermal characteristics of the design variables. The advanced procedure of the response surface method includes thermal characteristics of the design variables in a design range followed by changing each variable, x_i, in Eq. 1 into specially functional design variable, $f(x_i)$, as follow polynomial:

$$y = C_1 f(x_1)^2 + C_2 f(x_2)^2 + C_3 f(x_1) f(x_2) + C_4 f(x_1) + C_5 f(x_2) + C_6 \quad (2)$$

Subject to

$$f(x_i): \ \sin(x_i), \ldots, \ \log(x_i), \ldots, \exp(x_i),$$

etc.where $f(x_i)$ is determined through processes of understanding thermal characteristics. That is, the thermal characteristics are determined by survey of the research papers or numerical and experimental studies for each variable. In a result, the functional RSM has the principal advantages in terms of method a mechanism and approximation which are closer to the actual data compared to the non-functional RSM.

The overall procedures of the advanced response surface method with the functional design variables are presented in Fig. 2. Following steps are: (1) Select design variables and spaces in design parameters; (2) understand thermal characteristics by the variables; (3) construct design points using design of experiments (DOE); (4) perform experiments or numerical analyses; (5) perform regression analysis and analysis of variance (ANOVA); (6) create the approximation equations; (7) implement optimization processes to find the optimum values.

In the present study, the advanced RSM was used to obtain an optimal thermal design in an angled ribbed channel. The RSM is a term describing the collective use of DOE, regression analysis, and ANOVA. Unknown coefficients (C_i) of a second-order response surface polynomial have been determined by the least squares method. The set of design points was selected by the D-optimal method which provides an efficient approach for response surface model building as suggested by Mitchell [18]. It is known as a useful and reliable way of constructing a response surface with a small number of design points, such as only 1.5–2.5 times the number of unknown coefficients of the polynomial. As a result, it can save a large amount of computing time and resources, retaining the reliability of created response surface. When the observed response values are predicted accurately by the response surface model from the results of ANOVA, Myers et al. [15] and Guinta [16] suggested that the typical values of R^2_{adj} are in the range from 0.9 to 1.0. R^2_{adj} is an adjusted R^2 value in order to account for the degrees of freedom. The multiple determination coefficient (R^2) calculates the proportion of the variation in the response surface around the mean.

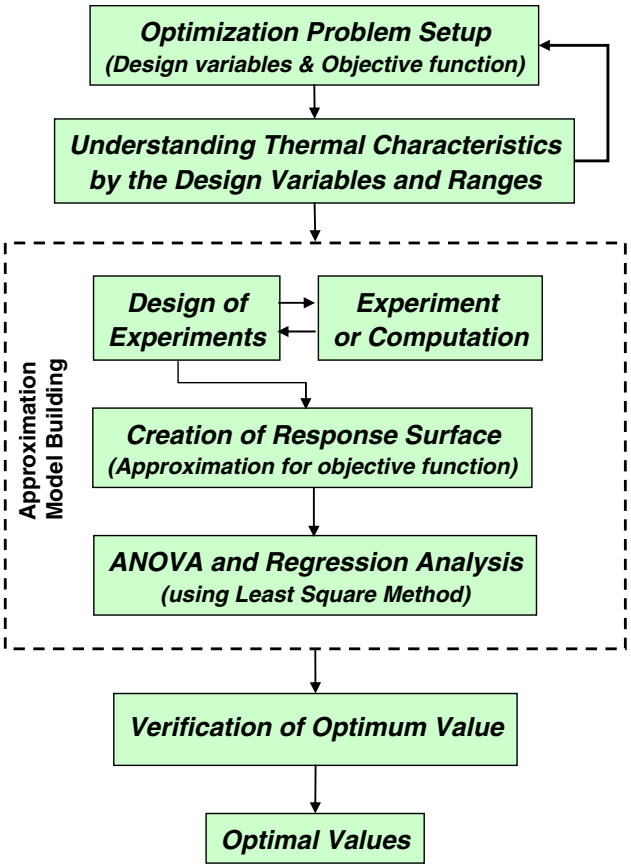

Fig. 2 Flowchart of the advanced response surface method processes

2.3 Design variables and objective functions

In a general angled channel with parallel rib arrangement, there are six parameters which are channel height (H), channel width (W), rib height (e), rib width (w), rib-to-rib pitch (p) and rib angle of attack (α). Among these parameters, the angled rib-induced the swirling flow and the rib-induced reattachment flow greatly affect the heat transfer enhancement. Therefore, we selected two design variables, rib angle of attack (α) and rib-to-rib pitch (p). The pitch is converted to a dimensionless variable, a ratio of rib-to-rib pitch-to-rib height (p/e). The design ranges are presented in Table 2.

Table 2 Design variables and ranges

Design variable	Lower bound	Upper bound
α (°)	30	80
p/e	3	15

To maximize pitch-averaged heat transfer and thermal performance, the objective function of heat transfer and thermal performance is defined as maximization of the following objective functions;

$$\mathrm{OF}_{\mathrm{Nusselt}} = \frac{\overline{Nu}}{Nu_0} \tag{3}$$

$$\mathrm{OF}_{\mathrm{TP}} = \frac{\overline{Nu}/Nu_0}{(f/f_0)^{1/3}} \tag{4}$$

where $\overline{Nu}$ is the pitch-averaged Nusselt number; and Nu_0 ($=0.023Re^{0.8}Pr^{0.4}$) is the Nusselt number obtained by Dittus and Boelter [19], which is for fully developed turbulent flows in a smooth pipe. The friction factor, f is calculated with the average pressure drop and f_0 represents the friction factor for a fully developed turbulent flow in a smooth pipe. The empirical equation that closely fits the Kármán–Nikuradse equation proposed by Petukhov [20] is employed as $f_0 = 2(2.236 \ln Re - 4.639)^{-2}$.

3 Results and discussion

3.1 Flow structure by rib turbulators

Figure 3 shows the flow structures and heat transfer distributions by the rib turbulators in stationary channels. For the case of a transverse rib arrangement (Fig. 3a), the high Nu ratios appear in an inter-rib region on the surface due to the transverse ribs. The peak appears at the upstream of the middle of the inter-rib region due to the reattachment of the flows passing over the ribs. For the case of an angled rib arrangement (Fig. 3b), the swirling flow is generated by angled ribs. By the impingement of the swirling flow, high Nu ratios on the downward flow region appear. However, the Nu ratios on the upward flow region become lower than that on the other regions, i.e., the angled rib turbulators generate the reattachment flow on the ribbed wall as well as the swirling flow induced along the rib angle of attack.

Figure 4 presents schematics of secondary flow structures near the wall; moreover, it shows the actual pitch related to heat transfer characteristics. The flow schematics are deduced from numerical calculations. The actual pitch is determined by two factors (the rib angle of attack and rib-to-rib pitch). For example, although the rib-to-rib pitch (p) is the same, the actual pitch is changed by the rib angle of attack (a) as shown in Fig. 4. It is because the direction and distance of secondary flow are induced by the combined effect. Furthermore, the rib angle of attack and a number of ribs change the strength and intensity of the secondary flow. The flow structures by two factors cause the heat transfer variation in angled ribbed channels.

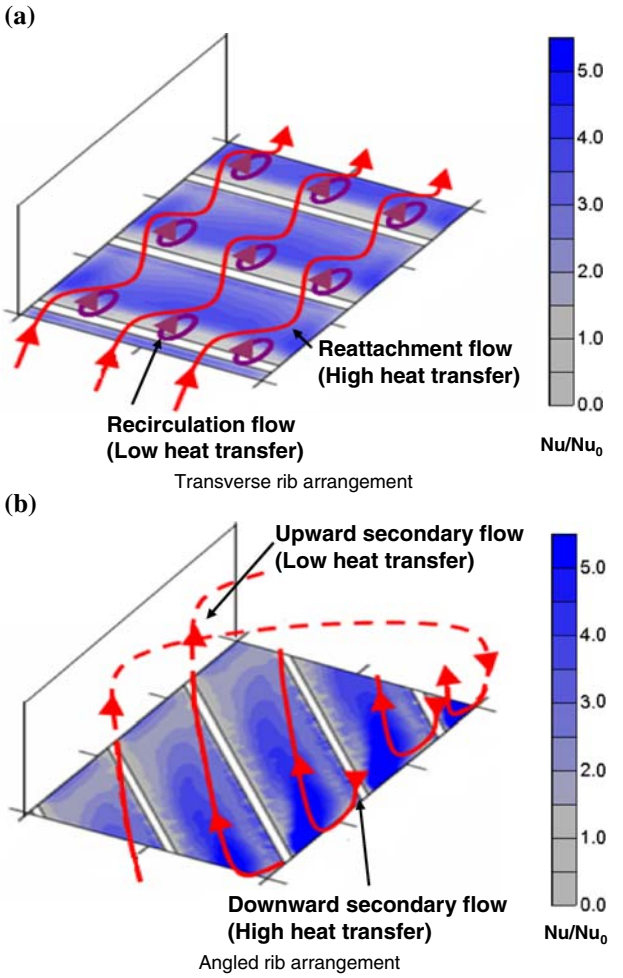

Fig. 3 Flow structures and heat transfer distributions induced by rib turbulators

3.2 Pitch-averaged heat transfer characteristics

Figure 5 presents the pitch-averaged Nusselt number ratio distributions in order to understand the heat transfer characteristics by rib angle of attack and rib-to-rib pitch. In addition, the present results were compared with the previous experimental data Han et al. [1], Cho et al. [2], Kim et al. [8], Liu [11]. As aforementioned, the angled rib turbulators generate the swirling flow that moves along the rib angle of attack, thereby enhance the heat transfer in inter-rib regions due to the impingement and the attachment of this flow. Thus, the swirling flow intensity and the heat transfer enhancement are strongly affected by the rib angle of attack. With increment of the rib angle of attack, the averaged values increase until for a specific angle (a) as shown in Fig. 5a. That is, when the specific angle is lower than 40° or higher than 70°, the flow intensity becomes weak; however, when the specific angle is between 40 and 70°, the flow intensity is strong. This tendency agrees reasonably with previous experimental data by Han et al.

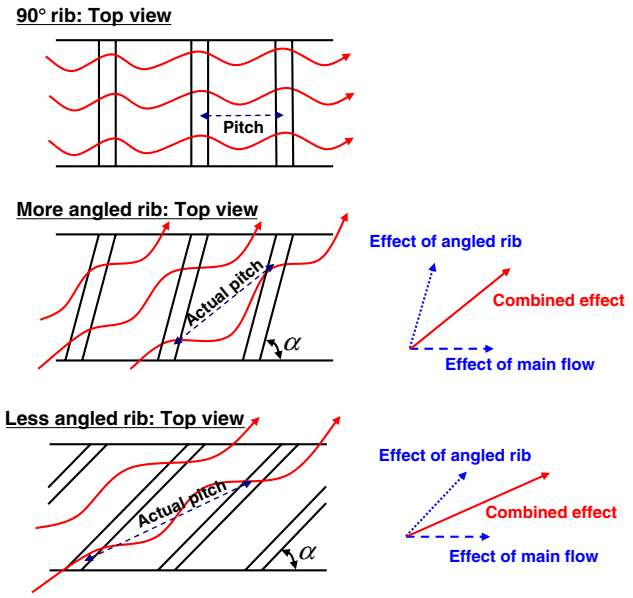

Fig. 4 Schematics of flow developed along rib angle of attack at constant pitch

[1] and Cho et al. [2] although the magnitudes of calculated *Nu* ratios are different from the experimental data reported by Kim et al. [8]. Figure 5b shows the effects of *p*/*e* on heat transfer at constant rib angle of attack of 45°. As *p*/*e* increases, the heat transfer increases until for a specific *p*/*e*. That is, until *p*/*e* increases to 5.0, the heat transfer increases. Thus, the heat transfer has a maximum value at *p*/*e* of 5.0. Among the averaged heat transfer values reported by Liu [11], the highest value also appears at $p/e = 5.0$, and the values decrease as the rib-to-rib pitch increases after this value. Although the different channel aspect ratio (*AR*) and rib height-to-channel height (*e*/*H*) result in different absolute heat transfer values, this tendency also agrees with numerical data.

3.3 Optimal thermal design

In the optimization, the resultant functions are composed of a second-order response surface which has six unknown coefficients at two design variables as presented in Eq. 1. The thermal characteristics of two design variables show distributions of logarithmic function as showed in Fig. 5. It is summarized as presented in Table 3. To estimate the unknown polynomial coefficients, design points have to be extracted within design ranges. Thus, using D-optimal method [18] and a design of experiments, 20 data points are selected. Based on the calculated results for these design points, the polynomial coefficients (C_i) are estimated by a least squares method. As a result, the Nusselt ratios and friction ratios are induced as Eqs. 5 and 6. In addition, the thermal performance is induced as Eq. 7.

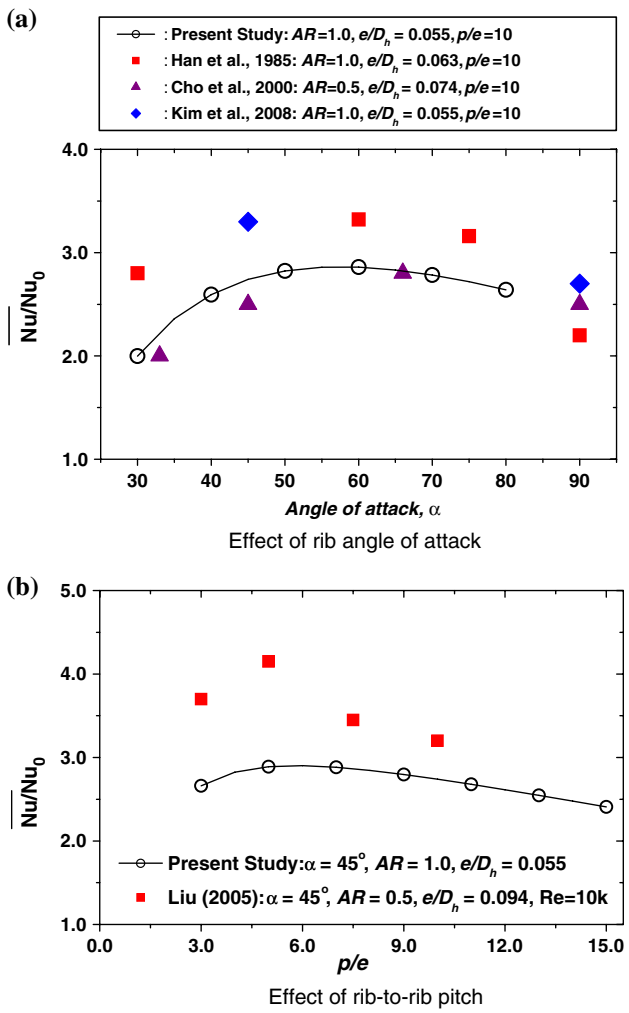

Fig. 5 Pitch-averaged Nusselt number ratios by each variable

Table 3 Summary of thermal characteristics by each variable

Variables	Results		
	Nusselt number ratio	Friction factor ratio	Thermal performance
x_1: α	$C_1[\log(x_1)]^2 + C_2\log(x_1) + C_3$		
x_2: *p*/*e*	$C_1[\log(x_2)]^2 + C_2\log(x_2) + C_3$		

−Averaged Heat Transfer ($R^2 = 0.957$, adj. $R^2 = 0.950$)

$$Nu/Nu_0 = -34.109 + 35.691\log(x_1) + 18.468\log(x_2) - 5.4061\log(x_1)\log(x_2) - 9.4844[\log(x_1)]^2 - 5.9187[\log(x_2)]^2 \quad (5)$$

−Friction Loss ($R^2 = 0.957$, adj. $R^2 = 0.951$) (6)

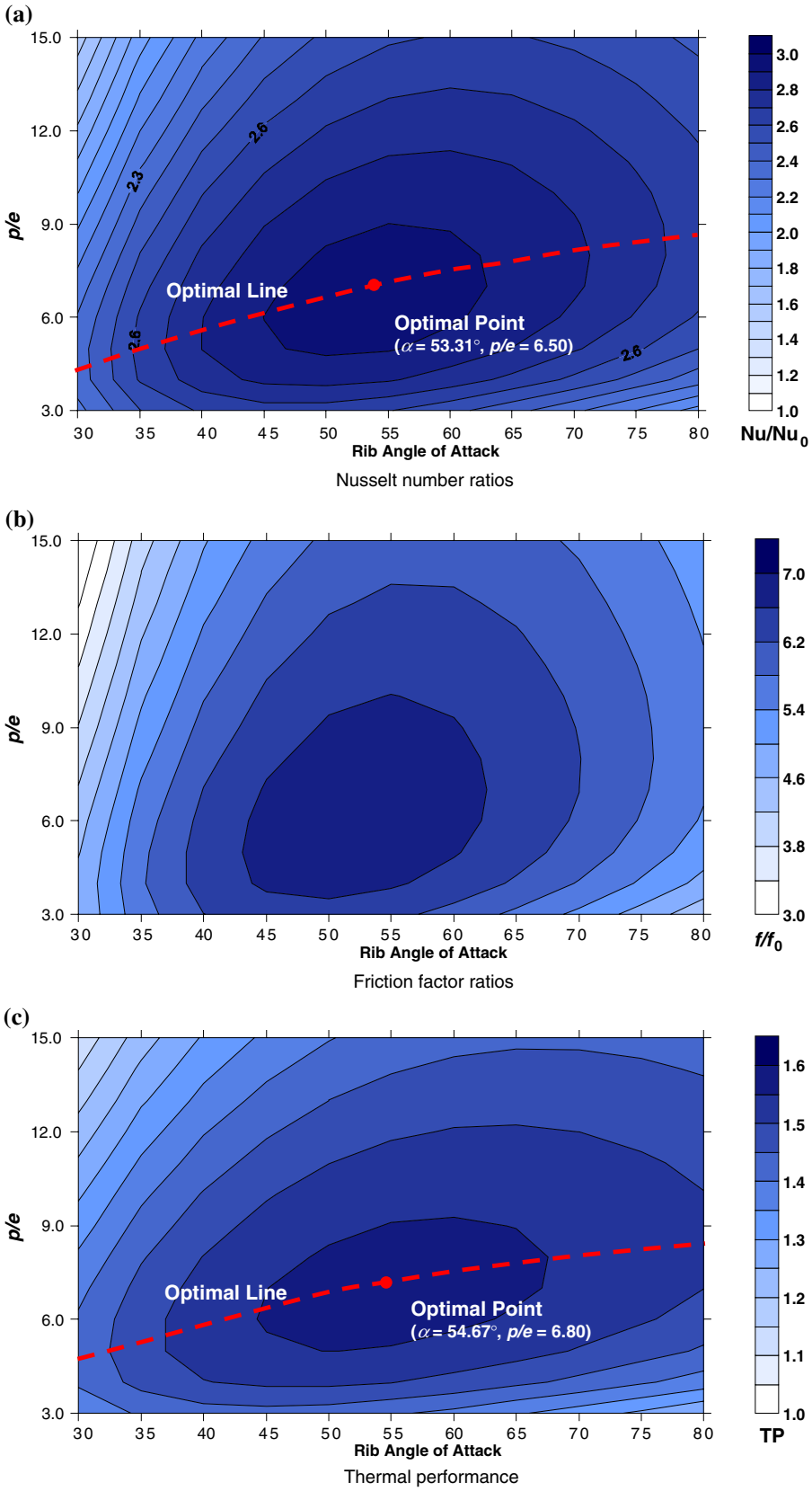

Fig. 6 Resultant maps for optimal thermal design

$$f/f_0 = -87.403 + 102.595\log(x_1) + 15.128\log(x_2) - 1.451\log(x_1)\log(x_2) - 29.563[\log(x_1)]^2 - 8.8499[\log(x_2)]^2$$

$-$Thermal Performance ($R^2 = 0.937,\ \text{adj.}\, R^2 = 0.927$) (7)

$$TP = -12.048 + 11.897\log(x_1) + 10.0671\log(x_2) - 3.2281\log(x_1)\log(x_2) - 2.9334[\log(x_1)]^2 - 2.833[\log(x_2)]^2$$

Figure 6 depicts the contour maps of pitch-averaged Nusselt number ratios (Fig. 6a), friction factor ratios (Fig. 6b), and thermal performance (Fig. 6c) for rib angle of attack and rib-to-rib pitch in Eqs. 5–7. The contour plot of the response surface was easily able to show the combined effects of two design variables in an angled ribbed channel. *Nu* ratios higher than 2.9 appear in ranges of $45° \le \alpha \le 65°$ and $5.0 \le p/e \le 9.0$. The optimum design point with the highest Nusselt number ratio appears at $\alpha = 53.31°$ and $p/e = 6.50$ and the highest thermal performance is at $\alpha = 54.67°$ and $p/e = 6.80$. Rib pitch (p/e) with maximum heat transfer in the angled ribbed channel is different from that in a 90° ribbed channel. It is noted that the aforementioned actual pitch is dominant in the angled ribbed channel. Optimum lines (rib pitch ratios, p/e with the highest heat transfer and the highest thermal performance at each rib angle of attack, α) are presented as following equations:

$$\text{Optimal Heat Transfer } p/e = -0.0003\alpha^2 + 0.1087\alpha + 1.4526 \quad (8)$$

$$\text{Optimal Performance } p/e = -0.0003\alpha^2 + 0.1036\alpha + 2.0368 \quad (9)$$

4 Conclusions

In the present study, the optimal geometries (rib angle of attack (a) and rib-to-rib pitch (p)) of angled rib turbulators was investigated to enhance the heat transfer and thermal performance by advanced response surface method based on approximation with functional variables using Reynolds-averaged Navier–Stokes analyses of fluid flow and heat transfer. The conclusions are summarized as follows:

1. Calculated pitch-averaged Nusselt number ratios showed reasonable agreement with previous experimental studies, fully enough to be used in the optimization process.
2. The actual pitch in the secondary flow direction decreased as the attack angle of angled rib turbulators increased; furthermore, the strength of the secondary flow was changed by the rib angle. The rib pitch with the maximum averaged heat transfer value was different at each rib angle of attack.
3. As a result of the optimization, the high regions of heat transfer and thermal performance induced by two design variables (α and p/e) appeared in ranges of $50° \le \alpha \le 60°$ and $6.0 \le p/e \le 7.0$. The highest heat transfer value was at $\alpha = 53.31°$ and $p/e = 6.50$ and the highest thermal performance was at $\alpha = 54.67°$ and $p/e = 6.80$.

Acknowledgments This work was supported partially by the Electric Power Industry Technology Evaluation and Planning Center.

References

1. Han JC, Park JS, Lei CK (1985) Heat transfer enhancement in channels with turbulence promoters. J Eng Turbines Power 107:628–635
2. Cho HH, Wu SJ, Kwon HJ (2000) Local heat/mass transfer measurements in a rectangular duct with discrete ribs. ASME J Turbomach 122:579–586
3. Taslim ME, Rahman A, Spring SD (1991) An experimental investigation of heat transfer coefficients in a spanwise rotation channel with two opposite rib-roughened walls. ASME J Turbomach 113:75–82
4. Rau G, Cakan M, Moeller D, Arts T (1998) The effect of periodic ribs on the local aerodynamic and heat transfer performance of a straight cooling channel. ASME J Turbomach 120:368–375
5. Astarita T, Cardon G, Carlomagno GM (1998) Average heat transfer measurements near a sharp 180 degree turn channel for different aspect ratios. IMechE Conf Trans: In: Optical methods and data processing in heat and fluid flow, London, UK, pp 137–146
6. Lau SC, Kukreja RT, McMillin RD (1991) Effects of V-shaped rib array on turbulent heat transfer and friction of fully developed flow in a square channel. Int J Heat Mass Transf 34:1605–1616
7. Kim KM, Kim YY, Lee DH, Rhee DH, Cho HH (2007) Influence of duct aspect ratio on heat/mass transfer in coolant passages with rotation. Int J Heat Fluid Flow 28:357–373
8. Kim KM, Park SH, Jeon YH, Lee DH, Cho HH (2008) Heat/mass transfer characteristics in angled ribbed channels with various bleed ratios and rotation numbers. ASME J Turbomach 130:031021
9. Han JC, Glicksman LR, Rohsenow WM (1978) An investigation of heat transfer and friction for rib-roughened surfaces. Int J Heat Mass Transf 21:1143–1156
10. Berger FP, Hau KF (1979) Local mass/heat transfer distribution on surfaces roughened with small square ribs. Int J Heat Mass Transf 22:1645–1656
11. Liu Y-H (2005) Effect of rib spacing on heat transfer and friction in a rotating two-pass rectangular (AR = 1:2) channel. M.S. thesis, Texas A&M University, USA
12. Kim HM, Kim KY (2004) Design optimization of rib-roughened channel to enhance turbulent heat transfer. Int J Heat Mass Transf 47:5159–5168
13. Kim HM, Kim KY (2006) Shape optimization of three-dimensional channel roughened by angled ribs with RANS analysis of turbulent heat transfer. Int J Heat Mass Transf 49:4013–4022
14. FLUENT 6.2 User's Guide (2003) Fluent Inc., Lebanon, NY, USA

15. Myers RH, Montgomery DC (2002) Response surface methodology: progress and product optimization using designed experiments. Wiley, New York
16. Guinta AA (1997) Aircraft multidisciplinary design optimization using design of experimental theory and response surface modeling methods. Ph.D. thesis, Department of Aerospace Engineering, Virginia Polytechnic Institute and State University, USA
17. Kim KM (2008) Optimal design of heat transfer systems for enhancing thermal performance and preventing thermal damage. Ph. D. thesis, Yonsei University, Korea
18. Mitchell TJ (1974) An algorithm for the construction of D-optimal designs. Technometrics 20:203–210
19. Dittus FW, Boelter LMK (1930) Heat transfer in automobile radiations of tubular type. University of California, Berkeley, Publications in Engineering 2:443–461; 1985 reprinted in Int Commun Heat Mass Transf 12:3–22
20. Prabhu SV (1970) Advances in heat transfer 6. Academic Press, New York, pp 503–564